



Effect of a Weak Jet on a Strong Jet

S. Louaifi-Hamaili, A. Mataoui and M. Aksouh

Theoretical and Applied Fluid Mechanics Laboratory, University of Science and Technology Houari Boumediene – USTHB, Algeria

†Corresponding Author Email: amataoui@usthb.dz

(Received November 21, 2018; accepted February 23, 2019)

ABSTRACT

This paper investigates the influence of a weak-jet on the development of a turbulent axisymmetric strong jet. A parametric study is carried out to evaluate simultaneously the effect to the jets-spacing ($S/D=3$ and $S/D=7.5$) and their velocity ratios in range $0 \leq \lambda \leq 1$. The mixing phenomenon is studied numerically by the finite volume method using the 3D-RANS second-order model, which gives a good agreement with the available data. Three distinct regions of this type of jets interaction are evidenced. This study confirms that the jets spacing affects strongly the converging region and has a minor effect on the combining region. It is found that the weak jet attracts the strong jet and the combining region extends from $30D$ to $40D$ where the self-similarity of a single jet is obtained. The jet width decreases when velocity ratio and jets spacing augment. In the combining region, in comparison with the free jet, it is found that the addition of a weak-jet increases the decay rate of the centerline velocity.

Keywords: Two unequal Jets; Turbulence; Strong jet; CFD; Self similarity.

NOMENCLATURE

D	strong-jet diameter	x_i	points coordinate
d	weak-jet diameter	$y_{1/2}$	half width of the jet velocity
I_0	turbulence intensity		
k	turbulent kinetic energy	λ	Velocity ratio.
P	pressure	ε	dissipation rate of turbulent energy
Re	Reynolds number	ρ	fluid density
S	distance between the jets axis	ν	kinematic viscosity
U_{0d}	weak-jet velocity	ν_t	turbulent kinematic viscosity
U_{0D}	strong-jet velocity		
U_i, U_j	velocity components		
U_c	axial velocity		
$\overline{u_i u_j}$	Reynolds tensor	Subscripts	
u'	Longitudinal fluctuation	0D	strong-jet
		0d	weak jet
		max	maximum value

1. INTRODUCTION

This paper examines the interaction of a strong jet with a weak jet. The interactions of two or more jets exhibit more advantages than single jets, such as better homogeneity, combustion and noise reduction. In most non-premixed industrial gas burners, multijets are used to improve the quality of combustion and reduce emissions. Injectors design requires knowledge of the physical mechanism of the interaction of two jets. In most practical applications of multijets, circular

nozzles are more used than rectangular nozzles. The particular interest in the performance of industrial injectors motivates the development of new fuel injection strategies. Jets combinations are also encountered in aerodynamic devices during vertical take-off and landing operations.

Many studies of two parallel jets are also considered as essential for the development of jets noise attenuation knowledge. However, most works reported in the literature were interested on the mixing of parallel slot jets. Hence, the

fundamental characteristics of twin slot jets have been studied by Miller and Comings (1960), Tanaka (1974), Murai *et al.* (1976), Ko and Lau (1989), Lin and Sheu (1990), Nasr and Lai (1997a) and (1997b)), Durve *et al.* (2012), Hasegawa, and Kumagai *et al.* (2008), Anderson and Spall (2001). Nevertheless, a limited number of studies addressed the interaction of two non-equal jets (Elbanna, 1987; Fujisawa *et al.*, 2004; Hnaïen *et al.* (2018)). These studies mainly focused on the effect of velocity ratio, Reynolds number, turbulence intensity and nozzles spacing; upon the dynamical characteristics and the location of merging and combined points.

On the other hand, practical applications are not limited to twin slot jets, but often require twin or multiple round jets. Recently, several experimental investigations were conducted on twin jets and multijets such as those performed by Okamoto *et al.* (1985), Harima *et al.* (2005), Tadamoto *et al.* (1995), Meslem *et al.* (2011), Rathakrishnan *et al.* (1989), Buchlin, J. M. (2011), Yin *et al.* (2007), Sabareesh (2015), Zheng *et al.* (2016) and Bentarzi *et al.* (2018). Rathakrishnan *et al.* (1989) have shown that two identical jets completely merge at a distance of 30 diameters downstream their exits. Furthermore, they highlighted a decrease of the velocity magnitude when the distance between them is augmented. Yin *et al.* (2007) investigated the influence of Reynolds number on the development of round twin jets. The authors reported that the increase of Reynolds numbers leads to stronger jet interactions and higher levels of turbulent kinetic energy. They also confirmed that twin jets attract each other and their interference increases when their spacing is reduced.

Most of these studies have predicted the location of the merging and the combining points. Twin jets are also required for noise reduction (Tadamoto *et al.*, 1995; Yimer and Grandmaison, 2001; Boopathi *et al.*, 2015; Bhat, 1978).

A small number of studies devoted on the interaction of two non-equals round parallel jets are available. Tadamato *et al.* (1995) investigated by flow visualization and velocity measurements, the mixing characteristics of two under expanded parallel jets, in particular the effect of nozzle spacing on the locations of both merging and combining points. They found that the longitudinal vibration of the flow is influenced by the distance between the two jets. The influence of a "weak" jet on a strong jet for velocity ratio of 0.25, inside a narrow cavity of $0.5 \times 0.5 \text{ m}^2$ has been numerically investigated by Vouros *et al.* (2003). They discussed the flow properties in the self-similarity region and reported similar characteristics compared to those of free jets. For a confined area prolonged to thirty times of the diameter of the weak jet, Vouros *et al.* (2004) have experimentally and numerically determined the characteristics of two jets of different diameters. They have highlighted two maximums in the vicinity of the axis of each jet, and an increase of the turbulence quantities. The Bending model based on the

momentum balance of the round twin jets interaction was developed by Faghani and Rogak (2013). The trajectory and the attachment of the two jets were rightly predicted using Reichardt's hypothesis. This model is able to predict the interaction of converging, diverging, parallel and non-equal jets. Furthermore it is well adapted for the simulation of engines with multi-holes injectors.

Using 2D Laser Doppler Anemometry (LDA), Later, Vorous and Panidis (2008) have studied experimentally the problem of two unequal jets of velocity ratio of 0.25. The influence of the weak jet and its Reynolds number on a strong jet, were examined. It appears, based on the mean velocity profiles that the two jets are quasi-independent in the initial region. However, the turbulent normal stresses indicate that the characteristics of the weak jet have been varied, particularly for the low Reynolds number. Downstream, the two jets merge until 20D, while the weak jet influences the mean velocity versus Reynolds number. The measurements of fluctuations, skewness and flatness factors highlight the effect of the Reynolds number on the weak jet. In the merging region (at a distance of 30D), the profiles of velocities and fluctuations are comparable to those of a single jet. However, the evolution of the axial velocity and skewness factor indicate that the mixing is not yet complete. Baratian, Ghorghi and Smith (2012) experimentally examined the merging of two unequal round jets. They have found that the profiles of concentration merge before those of velocity. Besides, turbulent stresses and the merging distance remain independent from the momentum ratio of the two jets.

For the design of industrial burners, Strong and weak jet may be used since they provide a better mixing of air and fuel ensures a less polluting and efficient combustion device. Hamaili and Mataoui (2017) investigated heat transfer of the cooling of a strong-jet by a weak-jet for one value of velocity ratio of 0.25, by first order turbulence model. They have shown that the temperature profiles in the developed region are self-similar, with reversed profiles at $y/y_{1/2} = 1$ and the location of the point of maximum temperature remain unchanged for temperatures ratios ranging between 0.88 and 1.

The paper investigates computationally the three-dimensional turbulent flow of the interaction between a strong and a weak jet, by applying a second order, Reynolds-stress model (RSM). Its complements available works of Vorous *et al.* (2003 & 2008) and Louaifi - Hamaili and Mataoui (2017) for several velocity ratios ($0 \leq \lambda \leq 1$) for and two spacing of the two jets ($S = 3D$ and $S = 7.5D$) (Fig. 1).

2. METHODOLOGY

The flow is isotherm, fully turbulent and three-dimensional. It is assumed to be incompressible and steady in average. Gravity forces are neglected.

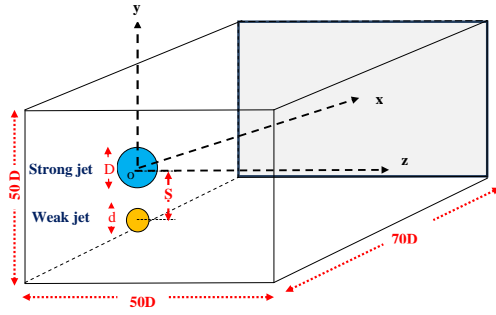


Fig. 1. Flow configuration and computational domain.

2.1 Governing Equations

The averaged equations are deduced from the conservation equations of mass and momentum coupled with the equations of the turbulence model. In this study, Reynolds Stress second order model (RSM) (Launder *et al.*, 1975) is used. It is based on the transport equations for each component of the Reynolds stress tensor $\overline{\rho u_i u_j}$ and the dissipation rate ε .

All simulations are performed by finite volume method (Patankar, 1980) which requires the transformation of all transport equations in conservative form to convection, diffusion and source terms (Eq. (1)).

$$\underbrace{U_j \frac{\partial \phi}{\partial x_j}}_{\text{Convection}} = \underbrace{\frac{\partial}{\partial x_j} \left(\Gamma_\phi \frac{\partial \phi}{\partial x_j} \right)}_{\text{Diffusion}} + \underbrace{S_\phi}_{\text{Source}} \quad (1)$$

Where ϕ is one of the dependent variables ($U_i, u_i u_j$ and ε). Γ_ϕ and S_ϕ are the corresponding diffusion coefficients and source terms, respectively. Diffusion coefficients and source terms of RSM (linear strain pressure version) model are given in Table 1.

All variables are interpolated using the POWER LAW scheme, except pressure that has been interpolated by the SECOND ORDER scheme. Pressure-velocity coupling is performed by SIMPLE algorithm.

At the exit of both jets, all variables are assumed to be constant. The two jets are parallel in x direction, with different velocities. For each jet, turbulent intensity I_0 is set at 6% and their dissipation rate is deduced from the macro-scale of turbulence corresponding to the jet diameter (Launder & Spalding, 1972):

$$\varepsilon_{0D} = \frac{c_\mu^{3/4} k_{0D}^{3/2}}{D} \quad \text{and} \quad \varepsilon_{0d} = \frac{c_\mu^{3/4} k_{0d}^{3/2}}{d}$$

where $C_\mu=0/09$, $k_{0D} = I_0 U_{0D}^2$ and $k_{0d} = I_0 U_{0d}^2$

All other boundaries are open at atmospheric pressure, where the pressure-outlet condition is imposed. They are chosen far from the area of the jets interaction in order to avoid their influences on the solution (Fig. 1).

Table 1 Diffusion coefficients and source terms of RSM model (Launder *et al.* (1975))

Φ	Γ_ϕ	S_ϕ
1	0	0
U_i	$\mu_{eff} = \mu_t + \mu$	$\left[-\frac{\partial p}{\partial x_i} + \frac{\partial}{\partial x_j} \left(\mu_{eff} \frac{\partial U_i}{\partial x_j} \right) \right]$
$\overline{\rho u_i u_j}$	$\mu \delta_{ij} + C_s \rho \frac{k}{\varepsilon} \overline{u_i u_j}$	$P_{ij} - \frac{2}{3} \delta_{ij} \rho \varepsilon + \Phi_{ij}$ $P_{ij} = -\overline{\rho u_i u_j} \frac{\partial U_j}{\partial x_k} - \rho u_j u_k \frac{\partial U_i}{\partial x_k}$ $\Phi_{ij} = \Phi_{ij,1} + \Phi_{ij,2}$ Where : $\Phi_{ij,1} = -\rho \varepsilon \left[C_{s1} a_{ij} + C_{s2} \left(a_k a_{ij} - \frac{1}{3} a_{mm} \delta_{ij} \right) \right]$ $\Phi_{ij,2} = -C_{t1} P a_{ij} + C_{t2} \rho k S_{ij} + C_{t3} \rho k S_j \sqrt{a_{mm} a_{mm}}$ $+ C_{t4} \rho k \left(a_k S_k + a_m S_m - \frac{2}{3} a_{ij} S_i \delta_j \right)$ $+ C_{t5} \rho k (a_k \Omega_k + a_m \Omega_m)$ With: $a_{ij} = \frac{u_i u_j}{k} - \frac{2}{3} \delta_{ij}$; $S_j = \frac{1}{2} \left(\frac{\partial U_j}{\partial x_i} + \frac{\partial U_i}{\partial x_j} \right)$ $\Omega_j = \frac{1}{2} \left(\frac{\partial U_i}{\partial x_j} - \frac{\partial U_j}{\partial x_i} \right)$
ε	$\mu \delta_{ij} + C_\varepsilon \rho \frac{\varepsilon}{k} \overline{u_i u_j}$	$\frac{\varepsilon}{k} (C_{\varepsilon 1} P_k - C_{\varepsilon 2} \rho \varepsilon)$ $P_k = -\overline{\rho u_i u_j} \frac{\partial U_i}{\partial x_j}$
Constants model		
$C_\mu=0.09$; $C_\varepsilon=0.18$; $C_{s1}=1.44$; $C_{s3}=1.92$; $C_{s1}=1.8$; $C_{s2}=0.6$; $C_{t1}=0.9$; $C_{t2}=0.8$; $C_{t3}=0.65$; $C_{t4}=0.625$; $C_{t5}=0.2$		

An entirely hexahedral mesh is used for the whole domain. A sufficiently fine grid is managed near the two jets where very high gradient of all variables prevailed (Fig. 2). Different meshes sizes have been tested. The computational and detailed grid arrangements are reported in Fig. 2. To select a suitable grid, several grids are tested in Fig. 3 indicating that both Grids 4 and 5 give the best results. Hence, computations have been performed for a grid 4. Furthermore, the validation is carried out on the basis of the experimental results of Vorous *et al.* (2003 and 2008) (Fig. 4). A further validation with available experimental data of longitudinal fluctuation u' ($u' = \sqrt{uu}$) (Vorous *et al.* (2008), is represented in Fig. 5, showing a good agreement.

3. RESULTS AND DISCUSSIONS

The interaction of two parallel turbulent round jets of different diameters is investigated numerically, for several velocity ratios, λ and jet-to-jet spacing S . The strong-jet and the weak-jet diameters are respectively $D=1\text{cm}$ and $d=0.6\text{ cm}$, and two distances between their axis are considered $S=7.5\text{cm}$ and $S=3\text{cm}$. For a given strong-jet velocity U_{0D} , the weak-jet is varied such as:

$0 \leq \lambda \leq 1$, where $\lambda = U_{0d} / U_{0D}$. Reynolds number is based on the strong-jet characteristics (velocity and hydraulic diameter of the strong jet), as follows:
 $Re = \frac{DU_{0D}}{\nu}$, varying in range $13700 \leq Re \leq 54800$.

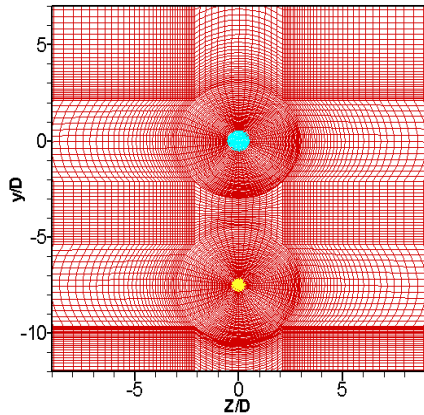
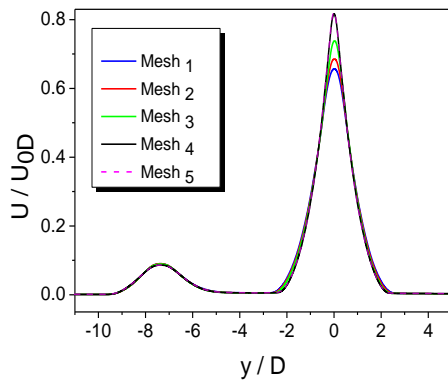
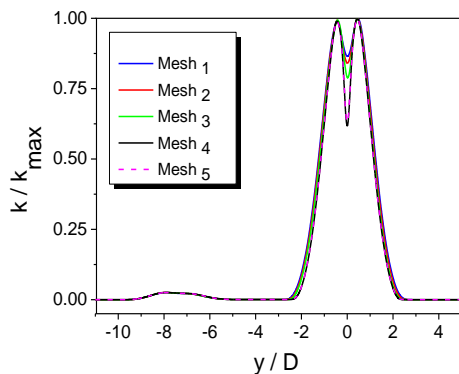


Fig. 2. Typical grid arrangement.

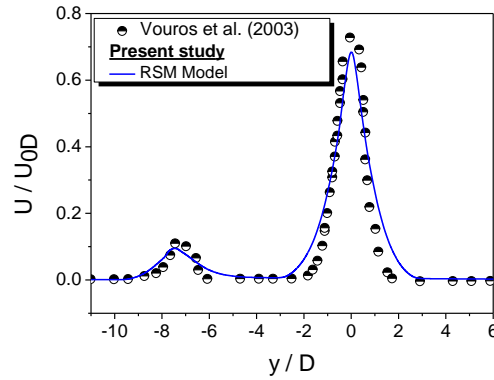


(a)

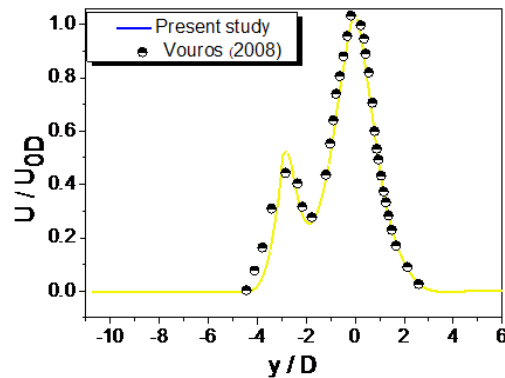


(b)

Fig. 3. Typical grid test ($\lambda = 0.25$).
 $Re_{0D} = 27400$, $Re_{0d} = 4100$, $X = 10D$, $Z = 0$
Mesh₁: 675012 nodes, Mesh₂: 1304359 nodes:
Mesh₃: 2628967 nodes, Mesh₄: 3959640 nodes and
Mesh₅: 4671175 nodes)
(a) Longitudinal velocity
(b) Turbulent kinetic energy



(a) $S/D = 7.5$



(b) $S/D = 3$

Fig. 4. Validation of mean velocity ($\lambda = 0.25$)
 $Re_{0D} = 27400$, $Re_{0d} = 4100$, $X = 10D$ and $Z = 0$.

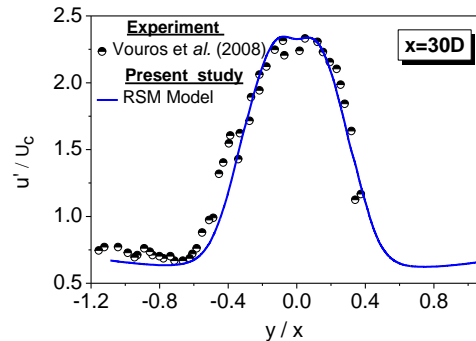


Fig. 5. Validation of longitudinal fluctuation.

3.1 Effect of Velocity Ratio and Jets Spacing

The contours of mean velocity are presented in Fig. 6 for $S/D = 7.5$ for two velocity ratios. Longitudinal velocity contours confirm the absence of any recirculation zone, in contrast to the case of slot jet configurations which generate several recirculation zones (Nouali & Mataoui, 2016; Wang & Hassan, 2015). This figure shows that the weak jet turn towards the strong jet for each velocity ratio. Downstream, the jets gradually combine inducing the structure of a single jet.

Figures 7 and 8, show the contours of U velocity component and kinetic energy in the initial region of the interaction. These two Figures evidence two pairs of obvious maximum for kinetic energy in the converging region in (x,y) plane (in the potential

core of the each jet) and have ringed shape in (y,z) plane. These maxima characterize the development of the shear layers that make up each jet, which gradually disappear downstream (outside the potential core of each jet). Moreover, downstream the initial region of the jets, the weak-jet begins to merge with the strong-jet, the peaks of kinetic energy vanish in the combining region where the structure of a single jet is obtained. Whilst small values of kinetic energy are obtained in the potential core area.

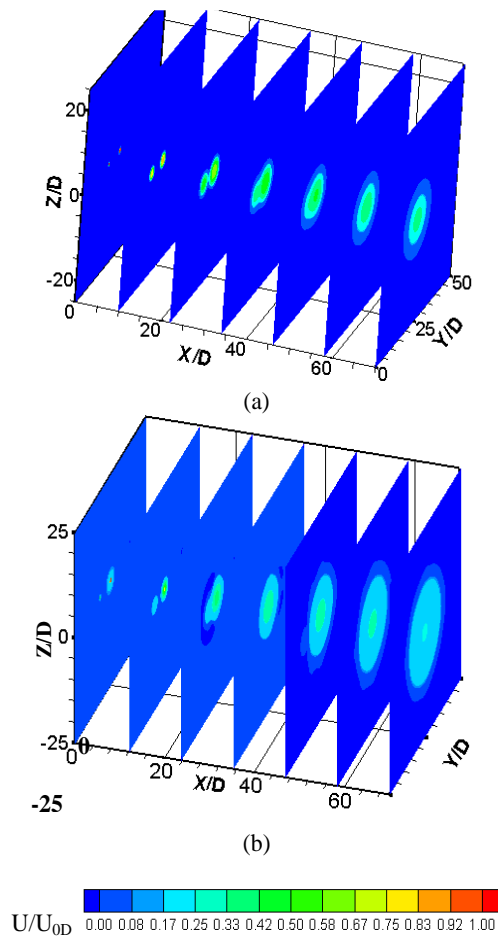


Fig. 6. Longitudinal velocity contours ($S/D=7.5$). (a) $\lambda=1$ and (b) $\lambda=0.25$.

In the convergence zone, the surrounding fluid is driven by the two jets, generating a negative pressure zone associated with Coanda effect.

For $\lambda=1$, the area of merging region extends to $x=35D$ for the case of $S/D=7.5$ (Fig. 8(a)) and to $x=25D$ for $S/D=3$ (Fig. 7(a)). Therefore, we can confirm that when the distance S between the two jets increases, the confluence point is shifted downstream along the x axis. Furthermore, the reduction of nozzles spacing enhances the mutual interaction of the inner layers of the two jets and induces an earlier merging.

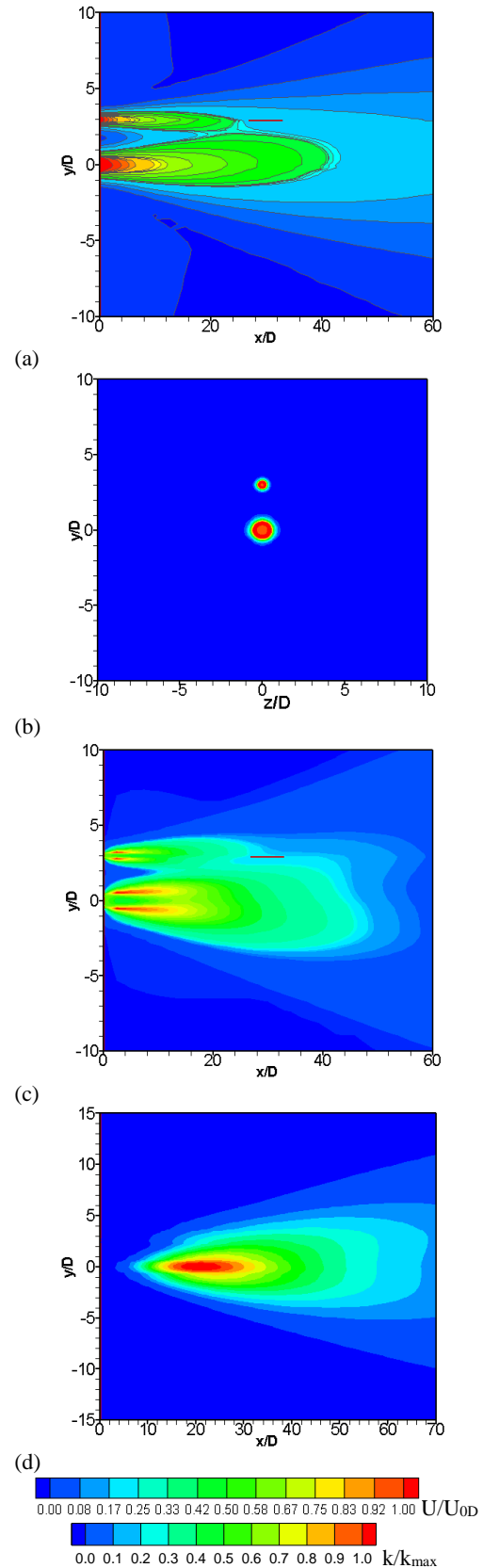


Fig. 7. Initial region ($\lambda=1$ and $S/D=3$) (a) U velocity component ($z=0.1D$), (b) Kinetic energy ($x=2D$) (c) Kinetic energy ($z=0$), (d) Kinetic energy ($z=2D$).

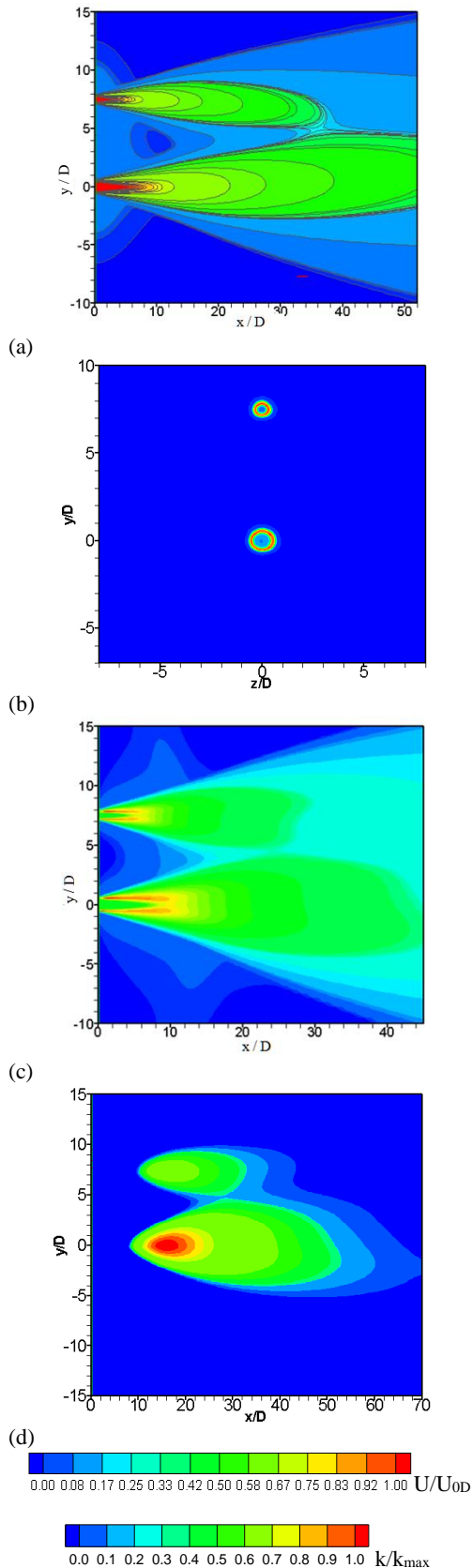


Fig. 8. Initial region ($\lambda=1$ and $S/D=7.5$)) (a) U velocity component ($z=0.1D$), (b) Kinetic energy ($x=2D$)) (c) Kinetic energy ($z=0$), (d) Kinetic energy ($z=2D$)

In the merging area, the pressure increases gradually

until a maximum value reached at the confluence point, where the two jets are fully combined and the structure of the single jet is obtained (Fig. 9). Pressure depends on the jets velocity ratio (λ) and the nozzles spacing (S). The analysis of this figure proves that the effect of S is dominant. The point of pressure maximum values matches with the confluence points, which vary greatly with S more than λ . So this figure shows clearly that the nozzles spacing S is related to the potential core length of the strong jet, which influences the longitudinal location of the confluent point.

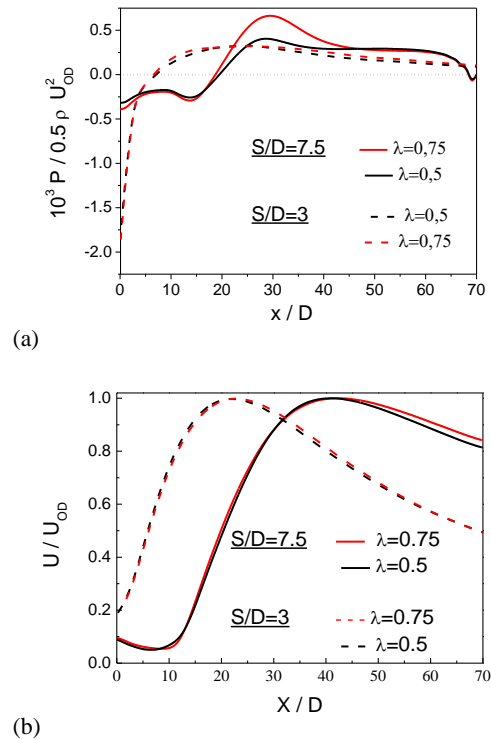


Fig. 9. Axial evolution of along the symmetric axis (a) Dimensionless pressure (b) Longitudinal velocity.

This figure proves that there is no negative longitudinal velocity U , associated with the absence of recirculation zones in the converging region. A maximum value of longitudinal velocity is observed for each nozzles spacing corresponding to the combining point where the weak jet is completely absorbed by the strong jet. Therefore the two jets combine each other to form a single self-similar jet. for velocity ratios $\lambda=0.75$ and $\lambda=0.5$, an increase of the jet spacing S induces a displacement of the confluence point and combining point further downstream along the longitudinal direction.

Distributions of Reynolds stresses contours (\overline{uu} , \overline{vv} , \overline{ww} , \overline{uv} , \overline{uw} , \overline{vw}) for $\lambda=0.25$ and $S/D=7.5$ are presented for several (x,z) plane of computational domain (Fig. 10). This figure highlights two main eddies corresponding to the strong-jet and the weak-jet, in the initial region ($x \leq 10D$). Great turbulence is highlighted along the shear layer developed by each nozzle edge and in the vortex ring core.

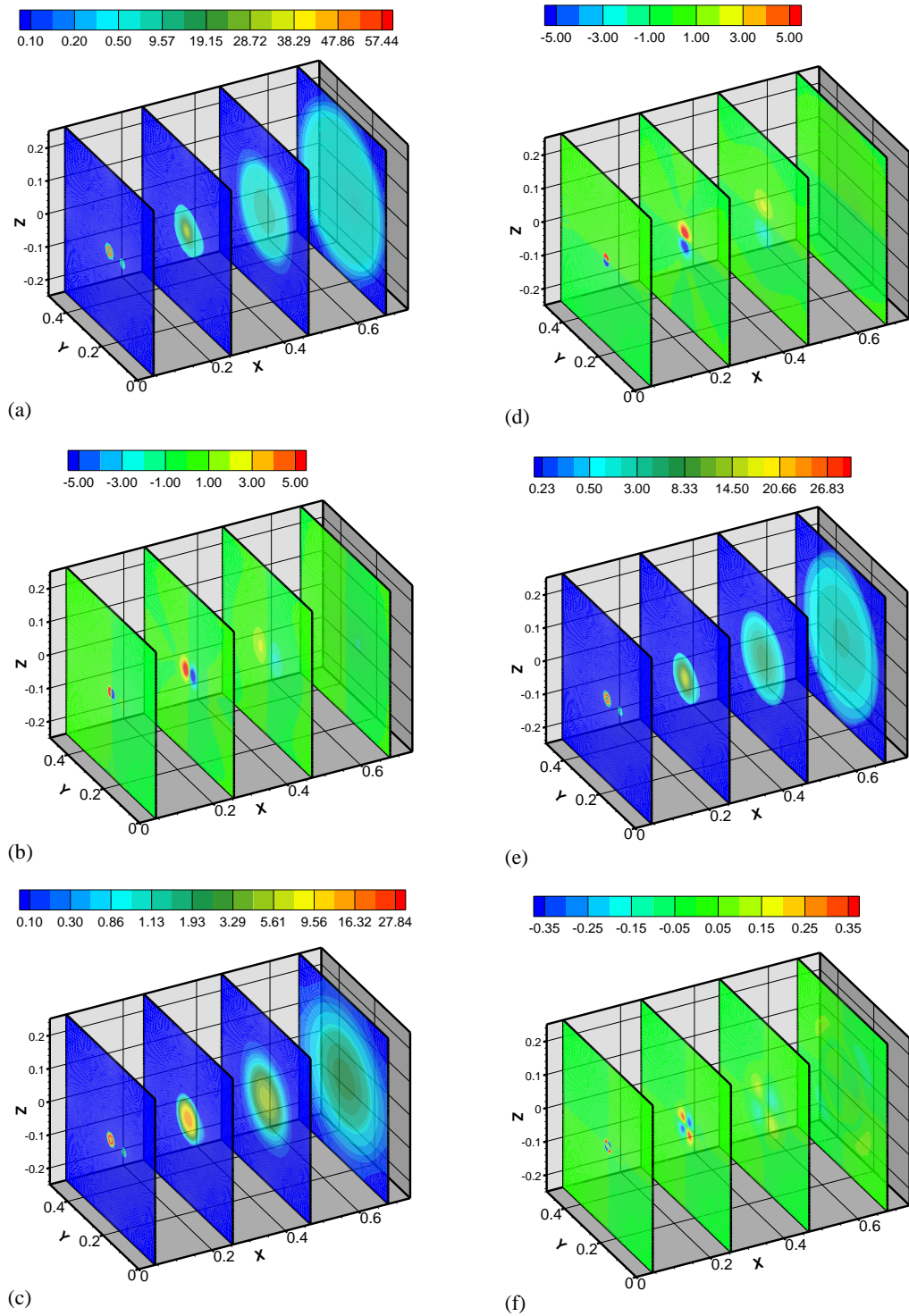


Fig. 10. Reynolds stresses contours (in m^2/s^2) ($\lambda=0.25$, $S/D=7.5$) (a) \overline{uu} , (b) \overline{vv} , (c) \overline{ww} , (d) \overline{uv} , (e) \overline{uw} , (f) \overline{vw} .

Downstream the initial region of the two jets, the weak-jet begins to merge with the strong-jet until the structure of a single jet is recovered. In (y,z) plane, the perpendicular stresses have ringed shape, and the cross stresses have symmetrical shape with opposite values associated with the sign of the Reynolds stress. It is positive in the upper outer-shear-layer and lower inner-shear-layer and negative in the upper

inner-shear-layer and lower-outer-shear.

3.2 Self similarity region

3.2.1 Effect of jet-to-jet spacing

In the self-similarity region, the single jet flow structure is recovered for each case of jet-to-jet spacing ($S/D=3$ and $S/D=7.5$). The crosswise

distributions $U(x-x_0)$ of the longitudinal velocity, (x_0 is the virtual origin of the strong jet) have similar shape for each jet-to-jet spacing (Fig. 12). This figure is a further comparison to validate the predicted results velocity profiles with the available data of [Wyganski & Fieler \(1969\)](#) for the case of a single free jet corresponding for $\lambda=0$. Figure 13 highlights the effect of jet-to-jet spacing on self-similarity velocity profiles, for a given velocity ratio.

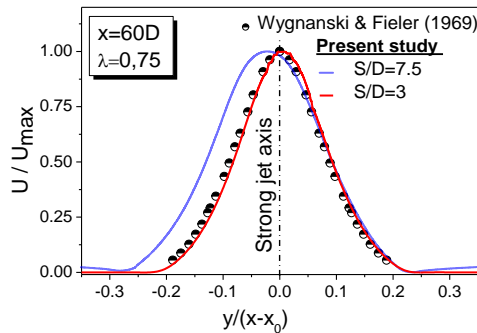


Fig. 12. Effect of jet-to-jet spacing on the crosswise distributions $U(x-x_0)$ of the longitudinal velocity.

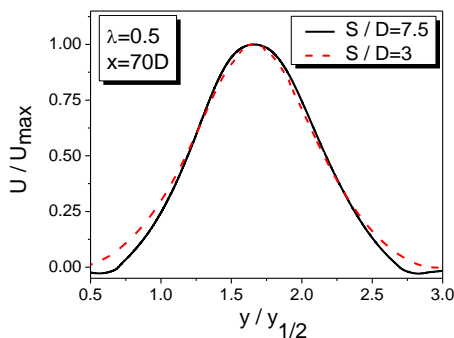


Fig. 13. Effect of jet-to-jet spacing on the self-similarity velocity profiles.

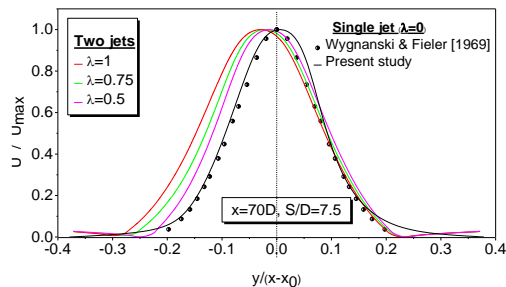
The influence of the velocity ratio is more visible on the side of the strong-jet (Fig. 14(a)) for the case $S/D=7.5$ than that of $S/D=3$ where the curves are practically superposed. Figure 14(a) shows that the position of maximum velocity (y_{max}) in case of $S/D=7.5$ is shifted from the strong jet axis since the entrainment rate increases for higher velocity ratio. It can be seen that the spreading of the strong jet in combining region exceeds that of the single jet. While for a smaller jet-jet spacing ($S/D=3$), it remains practically unchanged and the spreading of the jet is smaller than that of single jet (Fig. 14(b)).

In most available studies, it has been confirmed that the axial velocity follows a hyperbolic decay (far from the jet initial zone): $\frac{U_{0D}}{U_c} = \frac{1}{K_u}(x/D)$, U_c is

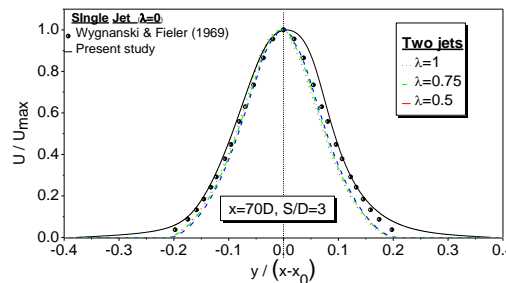
the centerline velocity, K_u is the rate of growth of the mean axial velocity. In this study, for $\lambda=0$, corresponding to the case of single jet, K_u is found of 6.2 close to available value of [Wyganski & Fieler \(1969\)](#) and [Hussein et al. \(1994\)](#). For $S/D=7.5$, Fig.

15(a) highlights the three region that characterize a round jet: inertial zone, transitional zone and self-similar zone. In the first two zones the curves are practically superposed for all velocity ratios. Furthermore, the development of the jet is virtually unaffected. [Pani and Dash \(1983\)](#) showed in the case of slot jet, that the decay rate of the mean velocity along the central jet decreases when increasing the number of jets. While for this study, the Fig. 15(b) shows in comparison with the single jet for $x > 50D$, the jet expands, therefore the decay rate K_u increases when the velocity of the weak-jet augments. So when the velocity ratio augments, the rate of growth K_u increases, justifying the effect of the weak-jet on the strong jet. The following correlation is obtained by fitting of computed data:

$$\frac{U_{0D}}{U_c} = (0,698 + 0,671 \lambda) + (0,15 - 0,0184 \lambda) \left(\frac{x}{D} \right) \quad (2)$$



(a)

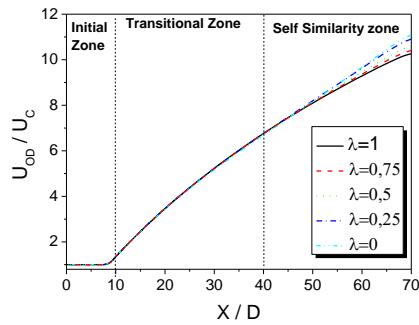


(b)

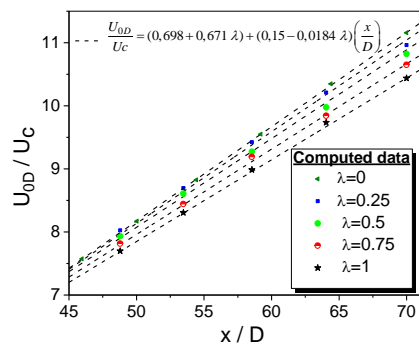
Fig. 14. Effect of jet-to-jet spacing on crosswise distributions $U(x-x_0)$ of the longitudinal velocity (a) $S/D=7.5$ (b) $S/D=3$.

Figure 16(a), shows the profiles of turbulent kinetic energy k/U_{0D}^2 along the strong-jet axis for different velocity ratios. Downstream of the jet exit, a sudden growth of the kinetic energy occurs by the effect of the development of the shear layers of the strong jet. Then, kinetic energy decreases gradually. All curves all superposed, this explains that turbulent kinetic energy of the strong jet is dominant and it is not affected for this range of velocity ratio ($0 < \lambda < 1$). In Fig. 16(b) illustrates the decay rate of the normalized turbulent kinetic energy along the central axis between the two jets at $y=3.75D$. A visible enlargement of curve for $\lambda = 0.25$ highlights the diffusion of turbulent energy throughout the interaction between the two jets. Furthermore, the

distribution of k/k_{max} reaches maximum value at $x/D = 30$ which agrees with the point of maximum pressure P_{max} .



(a)



(b)

Fig. 15. Axial evolution of dimensionless longitudinal mean velocity ($S/D=7.5$) (a) Along the x axis (b) In self-similarity zone.

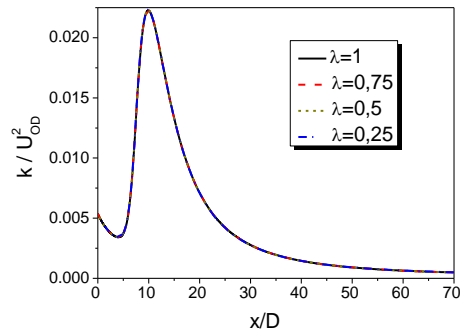
Figure 16(c), illustrates the ratio $(k_{max}/k)^2$ along the central axis between the two jets at $y=3.75D$. This figure shows that the far-field data are consistent with a linear relationship. The maximum is reached in range $10D < x < 20D$. Consequently, the kinetic energy is not strongly influenced by velocity ratio. This increase outcome from the high production of turbulence of the shear layers diffusion towards the central axis. A small difference is observed in the fully developed zone for low λ values.

4. CONCLUSION

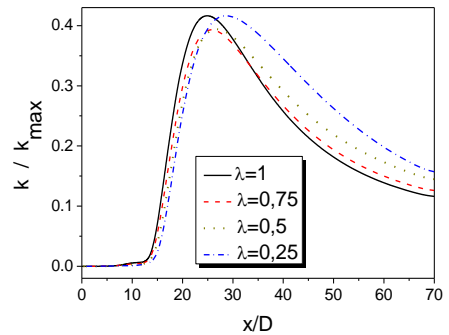
In this paper, the interaction of two isothermal, parallel, circular jets of different diameters is examined for two different jet-to-jet spacing, based on strong jet's diameter ($S = 3D$ and $7.5 D$).

The influence of jets velocity ratio λ that ranges from 0 to 1, is examined. A three-dimensional numerical simulation is performed using finite volume method. Regarding turbulence modeling, the Reynolds stress model accurately predicts this type of flow configuration. In the fully developed region, downstream of the confluence point, the velocity crosswise profiles are found similar. The deflection of the weak-jet toward the stronger jet along the perpendicular direction is associated with air entrainment generated by the Coanda effect. It

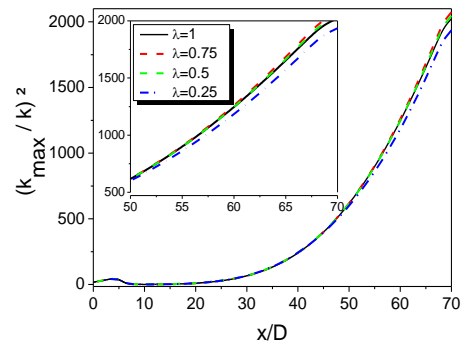
is also found that the addition of a weak-jet increases the decreasing rate of the centerline velocity. The decay rate of the velocity varies with the velocity ratio of the two jets. When the spacing between the two jets increases, the location of maximum velocity is shifted toward the side of the strong-jet. Therefore, the flow field induced by the two parallel round jets of different velocities becomes asymmetric in the area the strong jet centerline. Considering the large number of applications for which the flow field produced by the interaction of strong and weak jets is essential, in the prospects of this work the effects of additional geometrical parameters on the mean and turbulent characteristics of jets' mixing will be evaluated.



(a)



(b)



(c)

Fig. 16. Axial evolution of dimensionless turbulent kinetic energy ($S/D=7.5$) (a) Along the strong-jet axis (b) Along the central axis $y=3.75D$ (c) Ratio $(k_{max}/k)^2$ along the central axis between the two jets at $y=3.75D$.

REFERENCES

- Anderson, E. A., and Spall, R. E. (2001). Experimental and numerical investigation of two-dimensional parallel jets. *Journal of Fluids Engineering* 123(2), 401-406.
- Baratian-Ghorghi, Z., N. B. Kaye, A. A. Khan and J. R. Smith (2012). The merging of two unequal axisymmetric parallel turbulent jets. *Journal of Hydrodynamics* 24(2), 257-262.
- Benarzi, F., A. Mataoui, M. Rebay (2018). Effect of Inclination of Twin Jets Impinging a Heated Wall, *Journal of Applied Fluid Mechanics* 12(2):403-411.
- Bhat, W. V. (1978). Experimental investigation of noise reduction from two parallel-flow jets. *AIAA Journal* 16(11), 1160-1167.
- Buchlin, J. M. (2011). Convective Heat Transfer in Impinging-Gas-Jet Arrangements. *Journal of Applied Fluid Mechanics* 4(3), 137-149.
- Durve, A., A. W. Patwardhan, I. Banarjee, G. Padmakumar and G. Vaidyanathan, (2012). Numerical investigation of mixing in parallel jets. *Nuclear Engineering and Design*, 242, 78-90.
- Elbanna, H., &Sabbagh, J. A. (1987). Interaction of two nonequal plane parallel jets. *AIAA Journal* 25(1), 12-13.
- Faghani, E., and S. N. Rogak (2013). A phenomenological model of two circular turbulent jets. *International Journal of Engine Research* 14(3), 293-304.
- Fujisawa, N., Nakamura, K., and K. Srinivas (2004). Interaction of two parallel plane jets of different velocities. *Journal of Visualization* 7(2), 135-142.
- Harima, T., S. Fujita, and H. Osaka (2005). Turbulent properties of twin circular free jets with various nozzle spacing. In *Engineering Turbulence Modelling and Experiments* 6, 501-510.
- Hasegawa, H., and S. Kumagai (2008). Adaptive separation control system using vortex generator jets for time-varying flow. *Journal of Applied Fluid Mechanics* 1(2), 9-16.
- Hnaïen, N., Marzouk, S., Aïssia, H. B., & Jay, J. (2018). Numerical investigation of velocity ratio effect in combined wall and offset jet flows. *Journal of Hydrodynamics* 30(6), 1105-1119.
- Hussein, H. J., S. P. Capp and W. K. George (1994). Velocity measurements in a high-Reynolds-number, momentum-conserving, axisymmetric, turbulent jet. *Journal of Fluid Mechanics* 258, 31-75.
- Ko, N. W. M. and K. K. Lau (1989). Flow structures in initial region of two interacting parallel plane jets. *Experimental thermal and fluid science* 2(4), 431-449.
- Kolsi, L., N. Hnaïen, S. Marzouk, A. Al-Rashed, H. Ben Aïssia and J. Jay (2018). Numerical study and correlations development on twin-parallel jets flow with non-equal outlet velocities. *Frontiers in Heat and Mass Transfer (FHMT)* 11.
- Launder, B. E., and D. B. Spalding (1972). Mathematical models of turbulence. *Press: Academic, London and New York*, 19-33.
- Launder, B. E., Reece, G. J., &Rodi, W. (1975). Progress in the development of a Reynolds-stress turbulence closure. *Journal of fluid mechanics* 68(03), 537-566.
- Lin, Y. F. and M. J. Sheu (1990). Investigation of two plane parallel turbulent jets. *Experiments in Fluids* 10(1), 17-22.
- Louaifi-Hamaili S. and A. Mataoui, (2017). Interaction of Two Unequal Turbulent Jets with Different Temperature. *Heat Transfer—Asian Research* 46(7),961-977.
- Meslem, A., A. Dia, C. Beghein, M. El Hassan, I. Nastase and P. J. Vialle (2011). A comparison of three turbulence models for the prediction of parallel lobed jets in perforated panel optimization. *Building and Environment* 46(11), 2203-2219.
- Miller, D. R. and E. W. Comings, (1960). Force-momentum fields in a dual-jet flow. *Journal of Fluid Mechanics* 7(2), 237-256.
- Murai, K., M. Taga and K. Akagawa (1976). An experimental study on confluence of two two-dimensional jets. *Bulletin of JSME* 19(134), 958-964.
- Nasr, A. and J. C. S. Lai, (1997a). Comparison of flow characteristics in the near field of two parallel plane jets and an offset plane jet. *Physics of Fluids* 9(10), 2919-2931.
- Nasr, A. and J. C. S. Lai (1997b). Two parallel plane jets: mean flow and effects of acoustic excitation. *Experiments in Fluids* 22(3), 251-260.
- Nouali, N. and A. Mataoui (2016). Numerical analysis of steady turbulent triple jet flow with temperature difference. *Heat and Mass Transfer* 52(2), 315-330.
- Okamoto, T., M. Yagita, A. Watanabe and K. Kawamura (1985). Interaction of twin turbulent circular jet. *Bulletin of JSME* 28(238), 617-622.
- Pani, B. S. and R. N. Dash, (1983). Three-Dimensional Single and Multiple Free Jets, *Journal of Hydraulic Engineering ASCE*, 109(2), 254-269
- Patankar, S. V. (1980) *Numerical Heat Transfer and Fluid Flow*, McGraw-Hill, New York.
- Rathakrishnan, E., P. V. Reddy and K. Padmanaban (1989). Some studies on twin jet propagation. *Mechanics research communications* 16(5), 279-287.

- Reichardt, H. (1941), Über eine neue Theorie der freien Turbulenzen, *ZAMM*.
- Reichardt, H. (1942). Gesetzmäßigkeiten der freien Turbulenz. *VDI-Forschungsh.*, 414.
- Sabareesh, V. B., K. Srinivasan and T. Sundararajan, (2015). Acoustic characteristics of equal and unequal twin circular slot jets. *Journal of Sound and Vibration* 342, 90-112.
- Smith, J. R. W. (2008). *Investigation of the merging of two axisymmetric turbulent jets* (Doctoral dissertation, Clemson University).
- Tadamoto K; S. Mari; Y. Jinglong and M. Yoshihiro (1995). Interference Characteristics of Two Parallel Supersonic Jets Issuing from Pipes with Different Diameters. *Transactions of the Japan Society of Mechanical Engineers Series B* (61)588, 2968-2972.
- Tanaka, E. (1974). The interference of two-dimensional parallel jets: 2nd report, experiments on the combined flow of dual jet. *Bulletin of JSME* 17(109), 920-927.
- Vorous A., A. Yiannadakis and T. Panidis (2003). Round Jets Pairing. *3rd Meeting of the Greek Section of the Combustion Institute* University of Patras Conference Centre, 7-8 November, P2, 1-8
- Vouros, A., T. Giannadakis and T. Panidis (2004). Experimental Evaluation of a Basic Staged Combustion Configuration. *In Proc. Joint Meeting of Greek and Italian Sections of the Combustion Institute*.
- Vorous, A. and T. Panidis (2008). Influence of a secondary, parallel, low Reynolds number, round jet on a turbulent axisymmetric jet. *Experimental Thermal and Fluid Science* 32(8), 1455-1467.
- Wang, H., S. Lee and Y. A. Hassan (2015). Particle image velocimetry measurements of the flow in the converging region of two parallel jets. *Nuclear Engineering and Design* 306, 89-97.
- Wynanski, I. and H. Fiedler (1969). Some measurements in the self-preserving jet. *Journal of Fluid Mechanics* 38(03), 577-612.
- Yimer, I., H. A. Becker and E. W. Grandmaison (2001). The strong-jet/weak-jet problem: new experiments and CFD. *Combustion and Flame* 124(3), 481-502.
- Yin, Z. Q., H. J. Zhang and J. Z. Lin (2007). Experimental study on the flow field characteristics in the mixing region of twin jets. *Journal of Hydrodynamics, Ser. B* 19(3), 309-313.
- Zheng, X., X. Jian, J. Wei and D. Wenzheng (2016). Numerical and Experimental Investigation of Near-Field Mixing in Parallel Dual Round Jets. *International Journal of Aerospace Engineering*.